Tunable Waveguide Transmission Gratings Based on Active Gain Control

Mykola Kulishov, Victor Grubsky, Joshua Schwartz, *Student Member, IEEE*, Xavier Daxhelet, and David V. Plant, *Member, IEEE*

***Abstract*—Mode loss or gain can have a significant effect on the operation of waveguide transmission gratings as optical filters. Taking for example a long-period grating (LPG), we present a computer simulation that accounts for these effects. We show that cladding loss or gain result in qualitatively different LPG spectral behavior that can be used as a tuning mechanism in guiding structures where cladding mode properties can be controlled. One possible control mechanism is to have pump-driven gain in a doped cladding, which can perform gradual loss compensation and eventually gain excitement. Based on simulation results, we propose new approaches to tuneable amplifying filter designs in special fibers, as well as grating assisted co-directional couplers for integrated optics platforms.**

***Index Terms*—Gain control, gratings, lossy media, optical fiber amplifiers, optical fiber coupling, optical fiber filters, optical losses.**

I. Introduction

GROWING demand for the deployment of high-bandwidth services closer to the end customer will precipitate a new class of optical amplifiers for regional, metro-core, and metro-access networks. New and more complex loss/gain elements will be required to compensate for changes in amplifier operating conditions and channel load [1], [2]. Dynamically configurable midstage loss compensation will enable the use of a wider variety of loss components such as variable optical attenuators, and dynamic optical add-drop multiplexers with time-dependent spectral response. As we will demonstrate, waveguide transmission gratings can be created with certain dynamically tunable properties, which would make them well suited for these tasks.

Transmission gratings (TGs), such as long-period gratings (LPGs) in optical fibers [3], [4] are important elements for fiber-optic communications and sensor applications. In particular, they provide wavelength-selective light power exchange between co-propagating modes in so-called grating-assisted codirectional couplers (GACCs). For example, LPGs can be used for making wavelength-selective couplers and add-drop filters for coarse WDM systems [5]. A possibility to control grating properties would allow to dynamically change the coupling properties of such devices.

Because the resonance wavelengths of an LPG are sensitive to a number of physical parameters, such as mechanical strain, temperature, and the refractive index of the surrounding medium [6]–[9], various kinds of LPGS sensors and tuneable filters based of the shift in the resonance wavelength have been demonstrated. In all of these applications, the light energy coupled to the cladding mode is either absorbed and/or radiates away, or recoupled back into the core by the second LPG [10]. Despite of extensive experimental data, there has not been a consistent theory of lossy TGs that provided quantitative description of the loss influence on the grating transmissive and dispersive behavior.

Recently we have shown [11], that cladding mode losses play an important role in LPG operation, especially in the case of planar waveguide LPGs, where mode attenuation is ~0.1–1 dB/cm, which is significantly higher than in a standard single-mode fiber. These results prompted us to realize that having external control of the mode attenuation (through a mechanism like active pumping) adds a new dimension of the grating tunability. Pump power can be used to establish the spectral behavior of the grating by partially or fully compensating for the total losses or by introducing gain.

Although this TG tuning concept can be implemented in specially designed fibers, it is the planar waveguide platform that offers unique opportunities in combining electro-optic (EO) modulation in EO-materials with optical amplification [12], [13]. For example, by using polymer as an erbium host medium, a very high doping level of rare-earth atoms (more than 10^{26} atoms/m^3), which is at least 100 times higher than in silica glass [14], can be achieved without causing a significant ion-cluster effect. Usually, a compromise between the high erbium doping level and the parasitic effects of this doping is established to overcome intrinsic EO material losses and obtain a gain coefficient of at least several dB/cm with an acceptable length of doped optical waveguide. For example, An *et al.* [14] achieved 2 dB/cm gain at 1.06 μm with 22 pm/V of EO coefficient in a Nd^{+3}-doped chloride hexahydrate and chlorophenol red-based channel waveguide. This gain helps in compensating the high scattering and absorption losses of EO polymers.

We feel that a gap in the theory of waveguide grating exists in terms of TG behavior in an amplifying/attenuative environment. Although there has been extensive research [15]–[18] on reflection (Bragg) gratings with gain, (uniform, as well as π-shifted), we are not aware of any systematic study of gain effects on TG

Manuscript received February 13, 2004; revised August 11, 2004. This work was supported in part by the Natural Sciences and Engineering Research Council (NSERC) and industrial and government partners, through the Agile All-Photonics Networks (AAPN) Research Network.

M. Kulishov is with the Adtek Photomask Inc., Montreal, QC H4T 1J6, Canada (mkulishov@adtekphotomask.com).

V. Grubsky is with the Department of Physics, University of Southern California, Los Angeles, CA 90089 USA.

J. Schwartz and D. V. Plant are with the Department of Electrical and Computer Engineering, Photonic System Group, McGill University, Montreal, QC H3A 2A7, Canada.

X. Daxhelet is with the École Polytechnique de Montreal, Départment de Génie Physique et des Matériaux, Montréal, QC H3C 3A7, Canada.

Digital Object Identifier 10.1109/JQE.2004.836812

0018-9197/04$20.00 © 2004 IEEE

Authorized licensed use limited to: McGill University. Downloaded on February 23,2010 at 11:27:11 EST from IEEE Xplore. Restrictions apply.

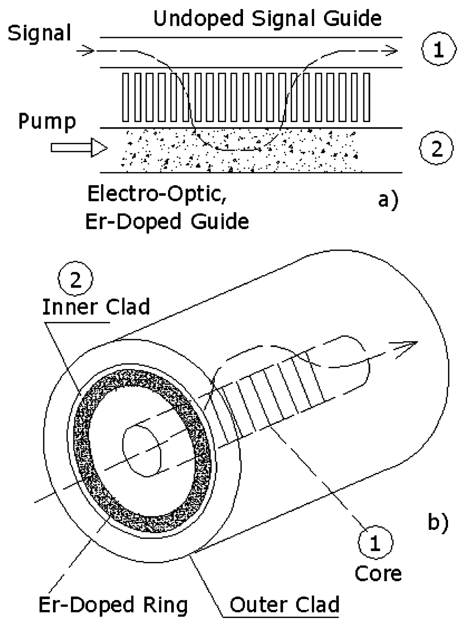

Fig. 1. General structure of an amplifying tunable filter based on (a) grating-assisted codirectional coupler and (b) long-period fiber grating.

transmission characteristics. Theoretical models [3], [4], [19] that are generally based on coupled wave equations do not account for mode attenuation/amplification. Partially this gap in LPG theory has been filled by our recent brief communication [11]. Here we provide more details to our analysis, extending it to include TG gain/loss behaviors for uniform and π-shifted refractive index profiles.

On the basis of our simulations we show how TG characteristics are affected by gain/loss factor in the cladding modes. In addition, we present new experimental results to support our theory. Based on the results of this analysis, a number of recommendations for GACC and LPG designs are provided.

II. Model Description and Possible Design Implementations

We suggest a TG filter, which allows to introduce loss or gain for one of the waveguide modes, shown schematically in Fig. 1 using either a planar waveguide, or a fiber configuration. Fig. 1(a) shows a proposed GACC implementation, where a TG provides coupling between two mismatched parallel guides.

The GACC can also be realized with an LPG made in a special fiber, for example by using so-called twin-core fiber [20] in which one core is doped with erbium, and the other core remains undoped. The TG written in such a fiber basically forms a codirectional coupler.

Alternatively, the loss/gain control of the cladding mode can be implemented in LPGs written in special rare-earth doped fibers. Schematic design of such fiber is presented in Fig. 1(b). Unlike traditional fibers in which the core is doped with rare-earth ions, the proposed design features a doped region around the core in the form of concentric ring with an internal radius exceeding the effective radius of the core mode [21]. Such fibers are often referred to as double-clad fibers. The pumping can be achieved through a large, multimode inner cladding that embraces the core, as well as the Er-doped ring. The pump light launched into the inner cladding has higher overlapping factor for signal cladding modes, than the signal core mode, that will result mainly in the cladding mode amplification without affecting the core mode. (Details on the pump techniques and fiber designs can be found in the literature [21]–[24]). At the same time, these cladding modes will suffer high losses if there is no pump provided.

Loss of the cladding mode can also be induced by applying a high-index material to the cladding surface and varying its refractive index [6], [10]. In practice, this could be accomplished with electrically controlled liquid crystal.

In the filter, the TG provides wavelength selective coupling of light from a low-loss signal guide 1 (or core for an LPG) with propagation constant $\beta_1 = \beta_1' + \alpha_1$ (β_1' here is the real part of the propagation constant; the loss of this mode can be neglected for simplicity, $\alpha_1 = 0$) into an Er-doped guide 2 (cladding) with the propagation constant $\beta_2 = \beta_2' + j\alpha_2$ where the light can be attenuated (without pump, $\alpha_2 > 0$) or amplified ($\alpha_2 < 0$) and returned back into guide 1. Guides 1 and 2 will henceforth be referred to as the undoped and doped guide, respectively.

For our calculations we use the following parameters for the TG model: effective indices of the modes are 1.487 068 and 1.48 for undoped and doped guides, respectively. To couple these modes at 1.555-μm wavelength, the TG has a period of 220 μm. These parameters are quite realistic for both proposed structures: the twin-core and the rare-earth-ring doped fibers. To model TGs, the preferred piecewise-uniform approach proceeds with identifying a fundamental matrix for each uniform section of the TG, and then multiplying these together to obtain a single matrix that describes the whole TG.

III. Transfer Matrix Equations

Our approach for calculating the properties of gratings with loss or gain is based on the coupled-mode theory [25]. This simplified approach is built on the assumption that the perturbation of the waveguide caused by the grating is sufficiently small, so that it does not change the modes significantly. This is true for typical long-period gratings in optical fibers, which explains why the experimental LPG results match the formulas of the coupled-mode theory very closely [3].

Although the coupled-mode theory is usually applied to modes with real propagation constants (no gain or loss), the basic equations are derived in a very general form [25] and therefore should hold even in the case when the propagation constants of one or both modes become complex. In other words, the interaction between modes with gain or loss will be correctly described by the standard coupled-mode equations if the real propagation constant β is replaced with a complex value $\beta + i\alpha$.

From the coupled-mode theory, light transmission in waveguides with a uniform TG can be described by a 2×2 transfer matrix T. In our case, the matrix relates the input undoped guide $R(z)$ and the doped guide $S(z)$ amplitudes at coordinate z with their respective amplitudes $R(z + L)$ and $S(z + L)$ at coordinate $z + L$, where L is the TG length. The elements of this transfer matrix are derived using coupled wave equations, and they can be found, in their most complete form, in the paper by

Authorized licensed use limited to: McGill University. Downloaded on February 23,2010 at 11:27:11 EST from IEEE Xplore. Restrictions apply.

Syms *et al.* [26]. The mode losses or pump-driven gains result in complex propagation constants, therefore, all phase factors that are neglected for loss-free models must now be carefully accounted for. We also account for the matrix dependence on the coordinate z at which the amplitudes $R(z+L)$ and $S(z+L)$ are presumed to be known. Usually $z=0$ for a uniform TG, however, in the case of abrupt phase discontinuities (so-called π-shifts) within the grating, or sampled TGs, the resultant matrix is a product of the individual matrices responsible for each uniform parts of the structure. In this case it is very important to provide the right initial coordinates. We use the matrix with the following elements:

$$\begin{aligned}
T_{11}(L,z) &= \left[\cos(\gamma L)+j\frac{\sigma}{\gamma}\sin(\gamma L)\right]\exp\left(j(\beta_1-\sigma)L\right)\\
T_{12}(L,z) &= j\frac{\kappa}{\gamma}\sin(\gamma L)\exp\left(j(\beta_1-\sigma)L\right)\exp\left(j\frac{2\pi}{\Lambda}z\right)\\
T_{21}(L,z) &= j\frac{\kappa^*}{\gamma}\sin(\gamma L)\exp\left(j(\beta_2+\sigma)L\right)\exp\left(-j\frac{2\pi}{\Lambda}z\right)\\
T_{22}(L,z) &= \left[\cos(\gamma L)-j\frac{\sigma}{\gamma}\sin(\gamma L)\right]\exp\left(j(\beta_2+\sigma)L\right) \qquad (1)
\end{aligned}$$

where κ is the cross-coupling coefficient, Λ is the grating period, and σ is the detuning factor. For our design, $\gamma=(\sigma^2+|\kappa|^2)^{1/2}$, and $\sigma=(\beta_1-\beta_2)/2-\pi/\Lambda$, where once again $\beta_1=\beta_1'+j\alpha_1$ and $\beta_2=\beta_2'+j\alpha_2$ are the complex propagation constants for the undoped and doped guides, respectively. The element T_{11} is responsible for the normalized light amplitude in the undoped guide, whereas T_{21} describes the signal amplitude for the doped guide. If light is launched only in the undoped guide at the input, the output signal power values are given by $P_1=|T_{11}|^2$ and $P_2=|T_{21}|^2$.

The group delay and dispersion of the transmitted light can be determined from the complex transmission amplitude $T_{11}(\mathrm{z})$ and $T_{21}(\mathrm{z})$. The phase response $\varphi(\omega)$ of the TG can be found as the argument of the complex amplitude. Alternatively, due to the causality of the TG response, the phase of the transmitted core mode can also be calculated as a Hilbert transform of $\ln(P_1)$, provided that the TG has no zeros in its spectrum [27]. Group delay τ and dispersion D can be identified, using the principle of Taylor series expansion, as

$$\tau=\frac{d\varphi}{d\omega}=-\frac{\lambda^2}{2\pi c}\frac{d\varphi}{d\lambda} \qquad (2)$$

$$D=\frac{d\tau}{d\lambda}=\frac{2\tau}{\lambda}-\frac{\lambda^2}{2\pi c}\frac{d^2\varphi}{d\lambda^2} \qquad (3)$$

measured in picoseconds and picoseconds/nanometers, respectively.

IV. Analysis of Mode Coupling in Presence of Loss or Gain

In the case of a grating without loss or gain ($\alpha_2=0$), the power transmitted through the undoped guide at the resonance wavelength ($\sigma=0$) is

$$P(L)=|T_{11}|^2=\cos^2(\gamma L) \qquad (4)$$

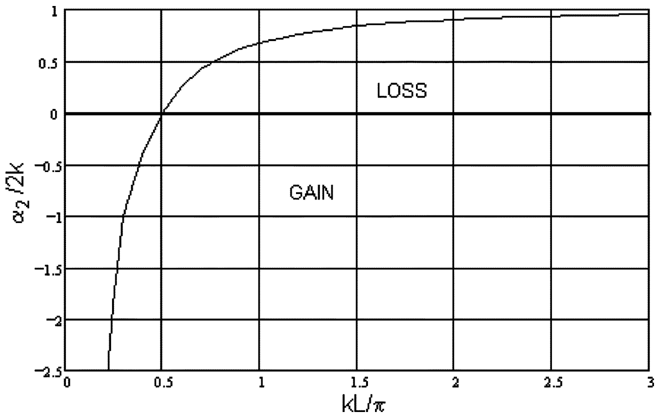

Fig. 2. Optimum loss or gain to coupling ratio $\alpha_2/(2\kappa)$ that provides 100% attenuation at the resonance wavelength for a given grating strength κL.

which means that light will be completely coupled into the mode of the doped guide at a distance $L=\pi/(2\kappa)$. At larger distance, the direction of coupling will reverse until all light comes back into the undoped guide. After that, the process will repeat cyclically, which was experimentally verified in the case of LPGs by measuring a grating transmission as a function of its length [28].

The interaction between modes becomes somewhat more complicated when either loss or gain for one of the modes (the mode of the doped guide in our case) is present. In this case, the resonance transmission of the TG becomes

$$P(L)=\left[\cos(\gamma L)+\frac{\alpha_2}{2\gamma}\sin(\gamma L)\right]^2\exp(-\alpha_2 L), |\alpha_2|<2\kappa \qquad (5a)$$

$$P(L)=\left[\cosh(\delta L)+\frac{\alpha_2}{2\delta}\sinh(\delta L)\right]^2\exp(-\alpha_2 L), |\alpha_2|\geq 2\kappa \qquad (5b)$$

where $\gamma=(\kappa^2-\alpha_2^2/4)^{1/2}$ and $\delta=(\alpha_2^2/4-\kappa^2)^{1/2}$. As shown in our previous work [11], there is an optimum value of losses that provides complete energy attenuation at the resonance wavelength in "over-coupled" gratings ($\kappa L>\pi/2$). Here we expand on that study by investigating the effects of both loss ($\alpha_2>0$) and gain ($\alpha_2<0$). The optimum attenuation condition can be obtained from the (5) by setting $P(L)=0$

$$\kappa L=\frac{\frac{\pi}{2}+\tan^{-1}\left(\frac{\frac{\alpha_2}{2\kappa}}{\sqrt{1-\left(\frac{\alpha_2}{2\kappa}\right)^2}}\right)}{\sqrt{1-\left(\frac{\alpha_2}{2\kappa}\right)^2}},\quad |\alpha_2|<2\kappa \qquad (6a)$$

$$\kappa L=\frac{2\kappa}{|\alpha_2|}\frac{\tanh^{-1}\left(\sqrt{1-\left(\frac{2\kappa}{\alpha_2}\right)^2}\right)}{\sqrt{1-\left(\frac{2\kappa}{\alpha_2}\right)^2}},\quad \alpha_2<-2\kappa. \qquad (6b)$$

Solving these equations, the optimum value of loss/gain can be found for a given L and κ. In Fig. 2 the solution of (6) is presented in dimensionless variables: κL and $\alpha_2/2\kappa$. For each value of κL the curve gives us the optimum ratio between the loss/gain value and the coupling coefficient that provides 100% signal attenuation in the undoped guide. As we can see from the plot, there is no solution for $\alpha_2/2\kappa>1$, i.e., it is impossible

Authorized licensed use limited to: McGill University. Downloaded on February 23,2010 at 11:27:11 EST from IEEE Xplore. Restrictions apply.

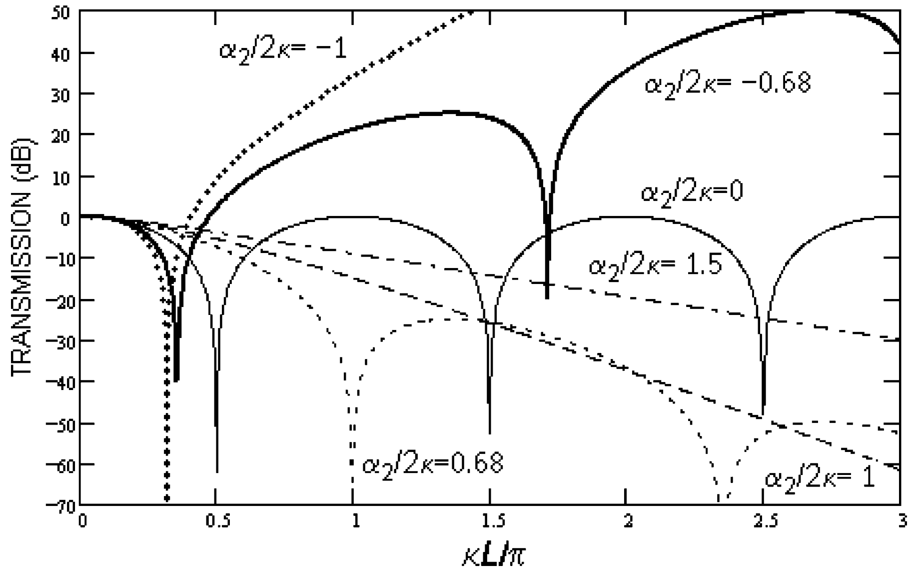

Fig. 3. Variation of the grating transmission at the resonance wavelength with the grating strength κL for different gain/loss parameter values.

to achieve full signal attenuation when loss becomes very high. However, losses allow us to provide 100% attenuation for any κL value of $\kappa L \geq \pi/2$ (over-coupled TG) and gain allows to reach 100% attenuation for any $\kappa L < \pi/2$ (under-coupled TG). This presents a new picture of the TG performance in which the shape of the transmission spectrum can be controlled by varying the mode loss or gain.

To provide some physical insight into the mode coupling process in the presence of gain or loss, we show the grating transmission as a function of κL for various values of $\alpha_2/2\kappa$. (Fig. 3). The conventional sinusoidal transmission of loss/gain-free grating is shown as a solid curve. We can clearly see distinct types of TG behavior depending on the magnitude of loss/gain.

A. Low to Moderate Loss $(0 < \alpha_2/2\kappa < 1)$

The TG exhibits periodic attenuation peaks, as in the loss-free case. However, in between the attenuation peaks, the transmission becomes progressively weaker along the TG length due to the absorption of the light in the doped guide. The attenuation peaks are spaced farther from one another and the first peak occurs at a longer TG length, than the loss-free case. This peak shift makes it possible to achieve the complete attenation for over-coupled TGs with $\kappa L > \pi/2$ by increasing the loss. For example, the dotted curve corresponding to $\alpha_2/2\kappa = 0.68$ shows how the total reversal of "full transmission" to "full attenuation" happens at $\kappa L = \pi$.

B. High Loss $(\alpha_2/2\kappa \geq 1)$

With high loss the light in the doped guide, the attenuation peaks disappear. Instead, we see a gradual, almost exponential decay of light intensity over distance. Perhaps counter-intuitively, the signal attenuation decreases as the loss goes up, as evident by comparing the curves corresponding to $\alpha_2/2\kappa = 1$ and $\alpha_2/2\kappa = 1.5$. It is easy to show that for $\alpha_2/2\kappa \geq 1$ the TG transmission can be approximated by

$$P(L) \approx \exp\left(-\frac{\alpha_2}{2}L\right). \tag{7}$$

This effect is due to the detuning factor σ becoming too large, which reduces the coupling efficiency into the doped guide faster than the loss increases. Practically any light coupled into the doped guide dissipates there and does not return back into the undoped guide.

C. Low to Moderate Gain $(-1 < \alpha_2/2\kappa < 0)$

Just as in the case of low loss, the evolution of the transmission over distance preserves periodic, equally spaced attenuation peaks. The peaks are spaced farther from one another and the first peak occurs at a shorter TG length when compared to the grain-free case. The peak shift makes possible complete attenuation for under-coupled TGs with $\kappa L < \pi/2$. In between the peaks, the light intensity gradually increases over distance.

D. High Gain $(\alpha_2/2\kappa \leq -1)$

Only the first attenuation peak now remains, as opposed to multiple, periodic peaks in the low-gain case. The peak continues to shift to shorter distance with increasing gain. The intensity of light increases almost exponentially with distance as we go away from the maximum attenuation distance $(L_{\max})$. In fact, one can show that for L $\gg L_{\max}$

$$P(L) \approx \exp\left(2|\alpha_2|(L - L_{\max})\right) \tag{8}$$

which means that the light in the both guides propagates with the same constant gain.

Authorized licensed use limited to: McGill University. Downloaded on February 23,2010 at 11:27:11 EST from IEEE Xplore. Restrictions apply.

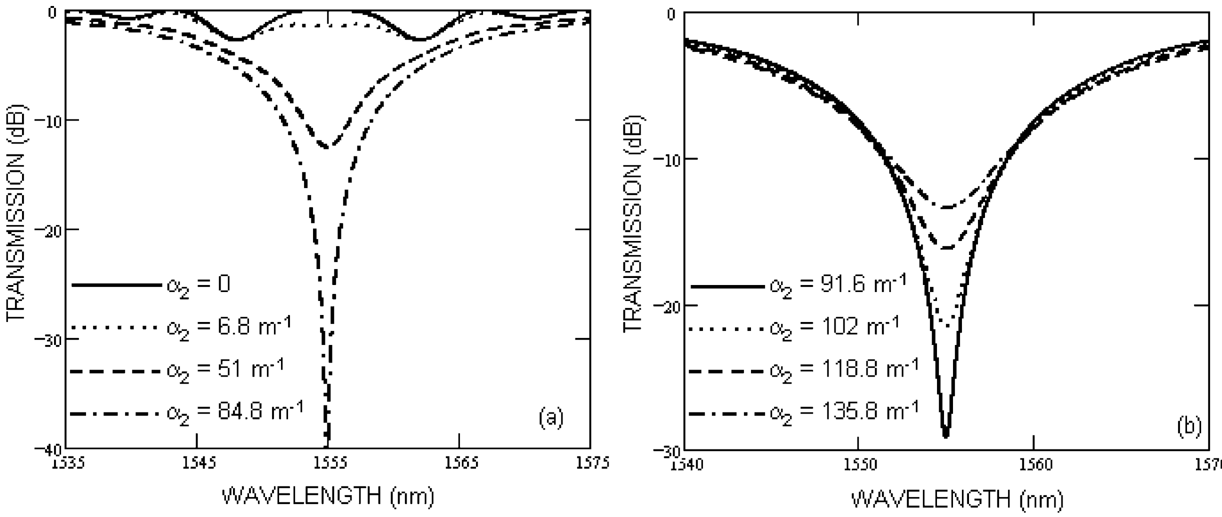

Fig. 4. Transmission spectra of the filter with $\kappa L = \pi$, $L = 50$ mm; $\kappa = 62.8\ \mathrm{m}^{-1}$ for the following cladding loss values: (a) $\alpha_2 = 0$ (solid); $\alpha_2 = 6.8\ \mathrm{m}^{-1}$ (dotted); $\alpha_2 = 51\ \mathrm{m}^{-1}$ (dashed); $\alpha_2 = 84.8\ \mathrm{m}^{-1}$ (dotted–dashed); (b) $\alpha_2 = 91.6\ \mathrm{m}^{-1}$ (solid); $\alpha_2 = 102\ \mathrm{m}^{-1}$ (dotted); $\alpha_2 = 118.8\ \mathrm{m}^{-1}$ (dashed); $\alpha_2 = 135.8\ \mathrm{m}^{-1}$ (dotted–dashed).

V. Simulations and Experimental Measurement of Grating Spectra

A. Spectrally Homogenous Gain/Loss

In this section we consider α_2 as a wavelength independent factor. This treatment is justified as long as the TG spectral bandwidth is much narrower than the gain spectrum for the Er^{3+} doped fiber. Small changes in the refractive index due to the pump will also be neglected. In addition, gain/loss distribution along the TG length is considered to be uniform.

1) Uniform Transmission Gratings: The TG spectra $(\kappa L = \pi)$ in Fig. 4(a) demonstrate how losses in the doped guide gradually evolve the spectrum from 100% transmission at the resonance wavelength (solid curve) for loss-free TG ($\alpha_2 = 0$, solid) to practically complete attenuation when the losses achieve its optimum value ($\alpha_2/2\kappa \approx 0.68$, dashed-dotted) in accordance with (6a). This spectrum evolution is accompanied by vanishing side-lobes. We call this loss value an "optimum" one, because further loss beyond this value leads to weaker rejections, as can be seen in Fig. 4(b).

It is interesting to note that the grating presence can speed up the light passing through it within the resonance wavelength, when $\alpha_2 < (\alpha_2)_{\mathrm{opt}}$, or vice versa to retard it when $\alpha_2 > (\alpha_2)_{\mathrm{opt}}$. This transitional point between retarding and accelerating optical transmission through the grating can be used to minimize the dispersion, as demonstrated in Fig. 5 where the dotted curve represents a transition between accelerating ($\alpha_2 < \alpha_{2\mathrm{opt}}$, dashed) and retarding ($\alpha_2 > \alpha_{2\mathrm{opt}}$, solid) TG regimes. The corresponding transmission spectra are plotted on a logarithmic scale in Fig. 5(a) for the losses $\alpha_2 = 95.2\ \mathrm{m}^{-1}$. This group delay distribution makes possible an extremely low dispersion level (less than 0.015 ps/nm) in Fig. 5(b) (dotted). This compares favorably to the dispersion level of 0.18 ps/nm for a loss-free TG with a similar attenuation level (−19.5 dB) and bandwidth, as shown by dotted–dashed curve in Fig. 5(a), where these spectra practically coincide. It must be noted that this low dispersion regime exists here at a substantial level of signal attenuation.

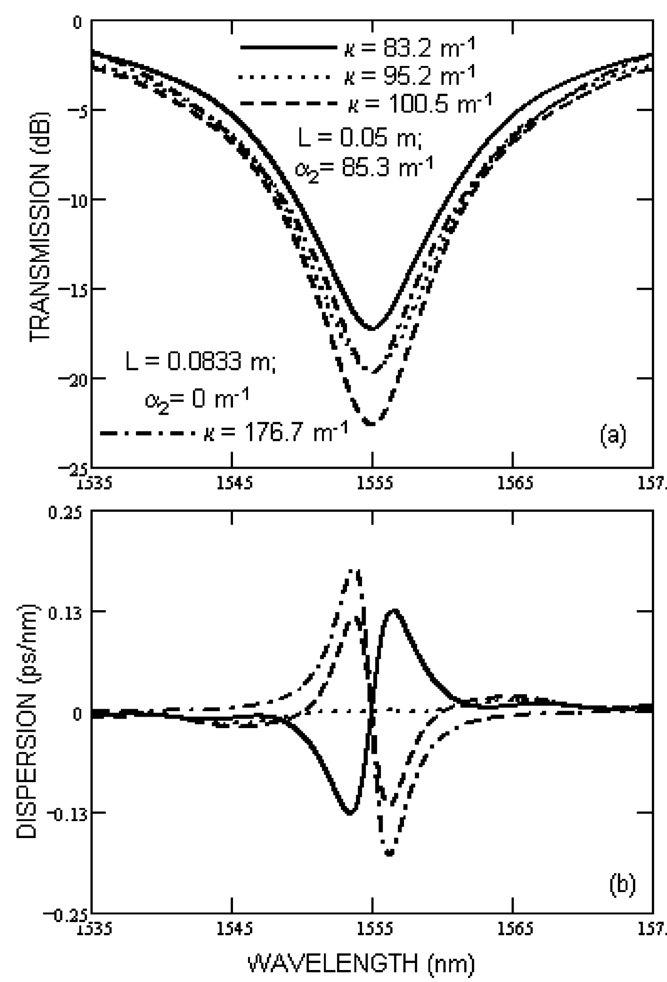

Fig. 5. (a) Transmission spectra and (b) dispersions of the filter with TG length $L = 50$ mm and $\alpha_2 = 85.3\ \mathrm{m}^{-1}$; $\kappa = 83.2\ \mathrm{m}^{-1}$ (solid); $\kappa = 95.2\ \mathrm{m}^{-1}$ (dotted); $\kappa = 100.5\ \mathrm{m}^{-1}$ (dashed); and $L = 8.33$ mm; $\alpha_2 = 0$; $\kappa = 176.7\ \mathrm{m}^{-1}$ (dotted–dashed).

In general the dispersion properties of TGs are uniquely related to their transmission spectrum of the core mode for

Authorized licensed use limited to: McGill University. Downloaded on February 23,2010 at 11:27:11 EST from IEEE Xplore. Restrictions apply.

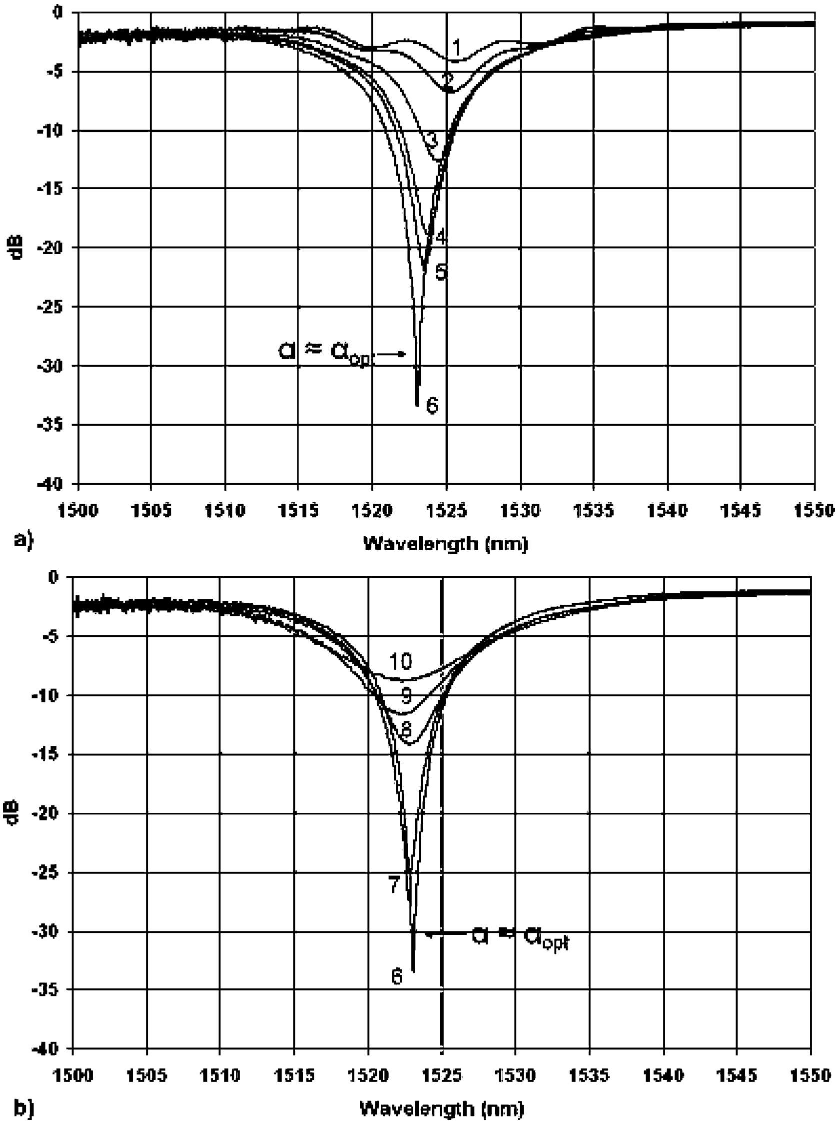

Fig. 6. Experimentally measured transmission spectra for LPG in fiber ($\Lambda = 220\ \mu$m, $\mathrm{L} = 50$ mm). (a) As cladding losses are increased (curves 1 to 6) using immersion in index solution with black ink, LPG attenuation at the resonance wavelength is also growing from 4 dB (no ink) to 34 dB. (b) After reaching the optimum level cladding mode losses, its further increase (curves 6 to 10) results in a decrease in attenuation to 9 dB.

the reason mentioned above. Therefore, filters with relatively broadband features in the transmission spectrum (such as LPGs) have very low dispersion (0.1–1 ps/nm). For this reason, in the subsequent discussion we will be paying attention mostly to the transmission spectra rather than dispersion.

In order to demonstrate the principle of loss-induced changes to TG spectral characteristics, a sample LPG was fabricated with a Ge-doped single-mode fiber. The grating was written with a spatial period of 220 microns using continuous-wave (CW) frequency-doubled Ar laser with a lasing wavelength of 244 nm to induce an estimated index change Δn of $\sim\ 3.5 \times 10^{-4}$. For this exposure, 100% transmission at the resonance wavelength of 1548 nm was achieved when the grating had a length of 50 mm. The LPG section was then suspended in a water-based solution of index approximately equal to that of the cladding ($n \approx 1.44$) at 1550 nm, essentially creating an infinitely thick cladding layer. The effect is to induce a substantial portion of the propagating cladding mode to propagate outside the physical fiber cladding, in the solution. Also, the resonance wavelength of the LPG shifts to approximately 1526 nm.

The water-based solution is already fairly absorptive at such wavelengths, and by adding an absorptive substance (in this case, carbon black ink) in suspension with the index-matched solution, we could effectively introduce further losses directly into the cladding mode. The results are shown in Fig. 6. As progressively more ink is added to the suspension, the transmission characteristics of the LPG change from a band-pass regime to band-stop at the resonance wavelength [Fig. 6(a)] as predicted by simulation. As further ink is added, the rejection weakens [Fig. 6(b)] as predicted by simulation for loss values exceeding the "optimal" level. Besides absorption, it is noted that the ink also changes the index of the surrounding solution, which is evident as a shift in the resonance wavelength from about 1526 nm in the cladding-matched case to 1522 nm. This is anticipated, because the index of ink is substantially higher than that of the solution. A comparative experiment consisting of the same LPG

Authorized licensed use limited to: McGill University. Downloaded on February 23,2010 at 11:27:11 EST from IEEE Xplore. Restrictions apply.

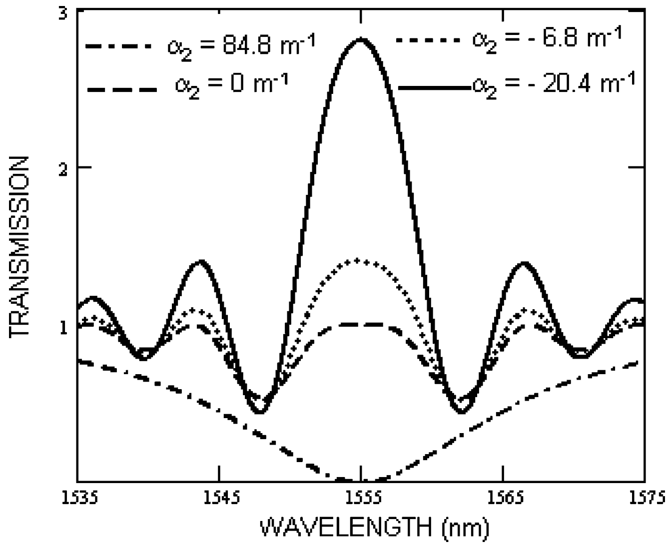

Fig. 7. Transmission spectra of the filter with $\kappa L = \pi$, $L = 50$ mm; $\kappa = 62.8$ m^{-1}; $\alpha_2 = 84.8$ m^{-1} (dotted–dashed); $\alpha_2 = 0$ (dashed); $\alpha_2 = -6.8$ m^{-1} (dotted); $\alpha_2 = -20.4$ m^{-1} (solid).

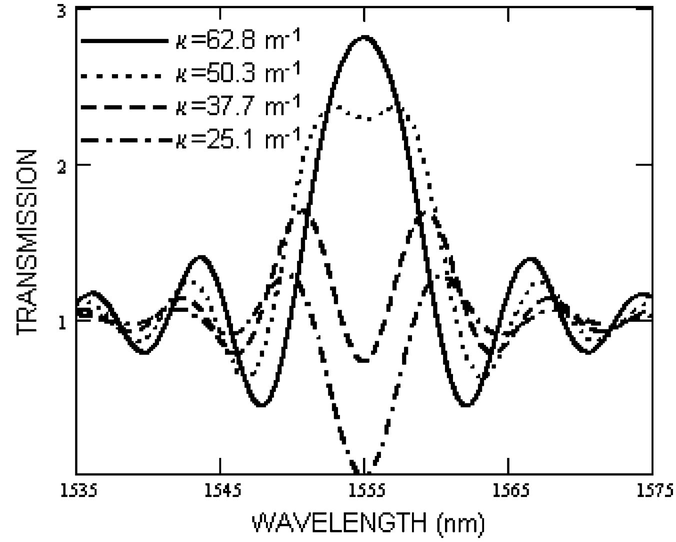

Fig. 8. Transmission spectra of the filter with the TG length $L = 50$ mm with gain $\alpha_2 = -20.4$ m^{-1}; $\kappa = 62.8$ m^{-1} (solid); $\kappa = 50.3$ m^{-1} (dotted); $\kappa = 37.7$ m^{-1} (dashed); $\kappa = 25.1$ m^{-1} (dotted–dashed).

submersed in ordinary water $(n = 1.33)$ showed us virtually no such response to ink because the cladding mode was still well confined to the physical cladding.

The effect of cladding mode loss on LPG spectrum was also studied before by Patrick *et al.* [6] and by Stegall and Erdogan [10]. In these works, the authors considered an LPG with initially 100% coupling $(\kappa L \approx \pi/2)$, which was then reduced and broadened by including variable loss for the cladding mode with high-index oils applied to the cladding surface. This behavior is in good agreement with our simulations shown in Fig. 3. In contrast with these works, here we show that, for a LPG with initially 100% transmission $(\kappa L = \pi)$, totally new behavior is possible—LPG attenuation increases with loss by over 30 dB. In addition, a new dimension of the LPG behavior could be explored by tuning loss and turning it into gain.

Fig. 7 demonstrates transmission characteristics for a uniform TG with strength $\kappa L = \pi$. Without pumping, the total loss level (total contribution of Er-ion absorption, material absorption and scattering) is set at the optimum value of $\alpha_2 \approx 1.36\kappa = 84.9$ m^{-1} $(\lambda = 1555$ nm$)$ or equivalently 7.4 dB/cm. This provides broadband attenuation (dotted–dashed curve). The transparency threshold is presented by the dashed curve $(\alpha_2 = 0)$, beyond which amplification takes place (dotted curve, $\alpha_2 = -6.8$ m^{-1} or 0.6 dB/cm; and solid curve $\alpha_2 = -20.4$ m^{-1} or 1.77 dB/cm).

The gain achievable in a standard fiber with Er^{3+}-doped core usually does not exceed 2–4 dB/m. However, higher levels of optical amplification become feasible in erbium-phosphate glass, where gain coefficients are on the order of 2–3 dB/cm [29]. Semiconductor based GACCs with gain exceeding 600 dB/cm and mode-beating lengths on the order of 15–20 μm [30] provide much opportunity for device design.

Fig. 8 demonstrates how the transmission evolves for a TG of fixed length (50 mm) and gain $(\alpha_2 = -20.4$ m$^{-1})$ with varying coupling coefficients. Such a device can be practically realized using electro-optically (EO) induced gratings [31]. The coupling coefficient is changed from $\kappa = 62.8$ m^{-1} $(\kappa L = \pi$, solid) to $\kappa = 25.1$ m^{-1} $(\kappa L = 0.4\pi$, dashed-dotted). It is interesting to note that practically complete attenuation at the resonance wavelength is achieved for this gain value at $\kappa L = 0.4\pi$ (more than -40 dB). As we explained earlier, complete power attenuation in the core guide with $\alpha_2 \geq 0$ can be achieved only at the TG strength $\kappa L \geq \pi/2$ (see Fig. 2). However, when using an actively pumped medium with a positive gain, complete mode attenuation is possible at $\kappa L < \pi/2$. The shorter the grating, the higher the gain must be in order to achieve full power transfer. For example, for the grating with strength $\kappa L = 0.25\pi$, complete transfer is achievable at $\alpha_2/2\kappa = -1.861$, i.e., $\alpha_2 = -46.7$ m^{-1} when $\kappa = 25.1$ m^{-1}. However, this strong attenuation at the resonance wavelength is accompanied by strong amplification in the two neighboring side-lobes.

2) Transmission Grating With a π-Shift: Phase shifts in TGs can drastically alter their transmission characteristics. For example, a π-shift introduced in the center of a uniform loss-free LPG with $\kappa L = \pi/2$ changes its spectrum from band-stop to a band-pass regime. Numerous publications on the phase-shifted LPG properties [32] describe them with the loss-free approximation, which is a fairly good one for the gratings written in standard fiber. The situation may be very different for TGs written, etched or electro-optically induced in GACCs, especially in planar waveguides where losses are much higher that in standard fibers. We are not aware of any quantitative study on phase-shifted TGs with losses (or gain) that would analyze their effect on TG performance. This analysis is particularly useful for devices with electro-optically induced TG where phase shift(s) can be easily introduced as well as easily removed in any place along the grating by simply reversing the applied voltage polarity for a portion(s) of the interdigitated electrode fingers [33].

Authorized licensed use limited to: McGill University. Downloaded on February 23,2010 at 11:27:11 EST from IEEE Xplore. Restrictions apply.

The transmission characteristics of a codirectional coupler with a π-shift that divides the grating into two parts with the lengths L_1 and L_2 $(L = L_1 + L_2)$ can be described by the matrix product: $T_R = T(L_2, L_1)I(\varphi)T(L_1, 0)$, where $I(\varphi)$ is the phase-shift matrix

$$I(\varphi) = \begin{bmatrix} \exp\left(\frac{j\varphi}{2}\right) & 0 \\ 0 & \exp\left(-\frac{j\varphi}{2}\right) \end{bmatrix}. \tag{9}$$

Using our matrix approach it is straightforward to get an expression for the signal amplitude in the undoped (core) and doped (clad) guides for the phase-shifted TG

$$\begin{aligned} T_{11}^{\pi} = & \frac{\exp\left(j(\beta_1-\sigma)L\right)}{\gamma^2} \\ & \times\left[\sigma^2\cos(\gamma L)\exp\left(\frac{j\varphi}{2}\right)+j\kappa^2\cos(2\gamma\Delta)\sin\left(\frac{\varphi}{2}\right)\right. \\ & \left.+j\sigma\gamma\sin(\gamma L)\exp\left(\frac{j\varphi}{2}\right)+\kappa^2\cos(\gamma L)\cos\left(\frac{\varphi}{2}\right)\right] \end{aligned} \tag{10}$$

$$\begin{aligned} T_{21}^{\pi} = & j\frac{\kappa^*\exp\left(j(\beta_2+\sigma)L\right)}{\gamma^2} \\ & \times\left[\gamma\sin(\gamma L)\cos\left(\frac{\varphi}{2}\right)+\sigma\cos(\gamma L)\sin\left(\frac{\varphi}{2}\right)\right. \\ & \left.-\left(j\gamma\sin(2\gamma\Delta)+\sigma\cos(2\gamma\Delta)\right)\sin\left(\frac{\varphi}{2}\right)\right] \end{aligned} \tag{11}$$

where $\Delta = (L_1 - L_2)/2$ is the distance of the phase shift location from the TG center. For a half wavelength phase shift $(\varphi = \pi)$ (10) and (11) are transformed into the following expressions

$$\begin{aligned} T_{11}^{\pi} = & j\exp\left(j(\beta_1-\sigma)L\right) \\ & \times\left[\frac{\sigma^2}{\gamma^2}\cos(\gamma L)+\frac{\kappa^2}{\gamma^2}\cos(2\gamma\Delta)+j\frac{\sigma}{\gamma}\sin(\gamma L)\right] \end{aligned} \tag{12}$$

$$\begin{aligned} T_{21}^{\pi} = & j\exp\left(j(\beta_2+\sigma)L\right) \\ & \times\left[\frac{\sigma\kappa}{\gamma^2}\left(\cos(\gamma L)-\cos(2\gamma\Delta)\right)+j\frac{\kappa}{\gamma}\sin(2\gamma\Delta)\right]. \end{aligned} \tag{13}$$

When there is no shift in the loss-free TG $(\Delta = L/2)$, the transmittivity is minimum at the resonance wavelength for the low grating strength values $(0 < \kappa\mathrm{L} \le \pi/2)$. The minimum reaches zero when the TG strength is equal to $\kappa L = \pi/2$. When a phase shift of π is introduced at the center of the TG, i.e., $\Delta = 0$, the minimum becomes a maximum with 100% transmission $(\sigma = 0, \gamma = \kappa)$ for an arbitrary κL value, and two rejection bands appear (dotted curve in Fig. 9). The TG strength has to be increased to $\kappa L = \pi/\sqrt{2}$ to achieve complete attenuation in these rejection bands. The losses in the doped guide reduce transmission at the resonance wavelength and increase transmission in the rejection band (solid and dashed curves in Fig. 9). On the contrary, gain in the doped guide produces a narrow-band amplification at the resonance wavelength, simultaneously increasing attenuation in the rejection bands (−15.5 dB attenuation for the dotted–dashed curve in Fig. 9). Comparing the amplifying spectra in Fig. 7 (solid) and Fig. 9 (dotted–dashed), one can say that π-shift introduction leads to narrowing the amplifying bandwidth with higher attenuation at the extremes.

For the situation of loss/gain in the doped guide, mismatch factor σ takes on a nonzero, purely imaginary value, $\sigma = -j\alpha_2/2$, which causes the normalized signal power in the undoped guide at the resonance wavelength to obey the following expression (in dimensionless variables $x = \alpha_2/(2\kappa)$ and $y = \kappa L$)

$$\begin{aligned} P = & \frac{\exp(-2xy)}{1-x^2}\left[\cos\left(2y\sqrt{1-x^2}\left(\frac{\Delta}{L}\right)\right)\right. \\ & \left.-x^2\cos\left(y\sqrt{1-x^2}\right)+x\sqrt{1-x^2}\sin\left(y\sqrt{1-x^2}\right)\right]^2. \end{aligned} \tag{14}$$

The transmission at resonance is therefore a function of the π-shift distance from the grating center (Δ/L), as it is shown in Fig. 10. When $\Delta/L = 0.5$, it means that π-shift is at the very end and the result is a uniform grating. The plot demonstrates that by moving the π-shift position from the center it is possible to gradually reduce amplification at the resonance wavelength and reach a position with zero transmission. An example of the spectrum control through the π-shift position is shown in Fig. 11, where transmission at the resonance wavelength is

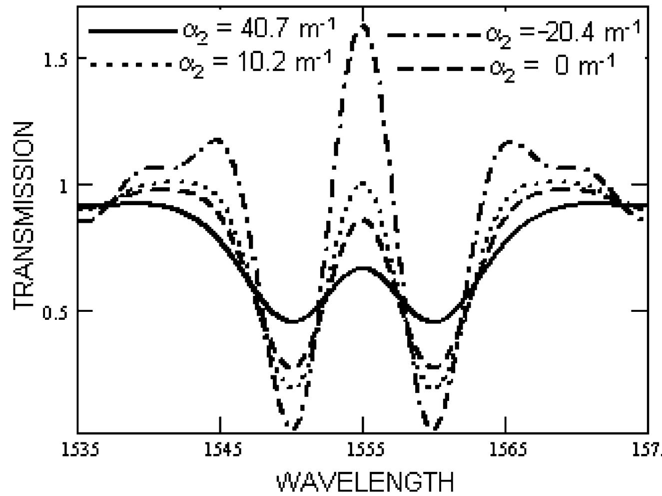

Fig. 9. Transmission spectra of the filter with π-shift in the middle of TG with $\kappa L = \pi/2$, $L = 50$ mm; $\kappa = 31.4$ m^{-1}; $\alpha_2 = 40.7$ m^{-1} (solid); $\alpha_2 = 10.2$ m^{-1} (dashed); $\alpha_2 = 0$ (dotted); $\alpha_2 = -20.4$ m^{-1} (dotted–dashed).

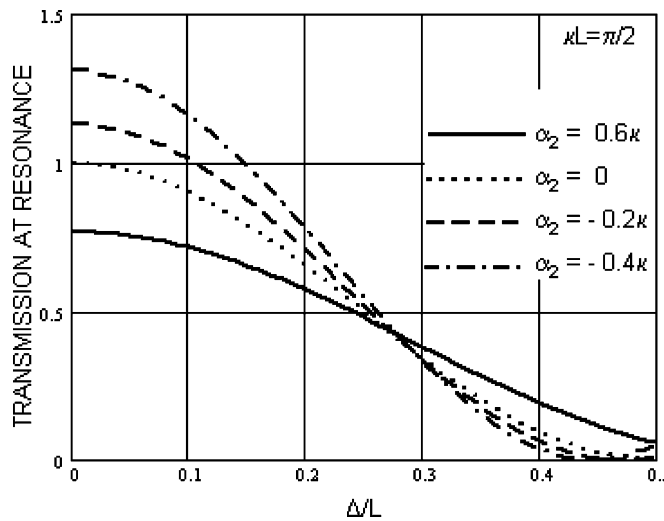

Fig. 10. Transmission at the resonance wavelength as a function of the relative π-shift distance from the TG center for the grating with $\kappa L = \pi/2$ and different value of the gain/loss factor: $\alpha_2 = 0.6\kappa$ (solid); $\alpha_2 = 0$ (dotted); $\alpha_2 = -0.2\kappa$ (dashed); $\alpha_2 = -0.4\kappa$ (dotted–dashed).

Authorized licensed use limited to: McGill University. Downloaded on February 23,2010 at 11:27:11 EST from IEEE Xplore. Restrictions apply.

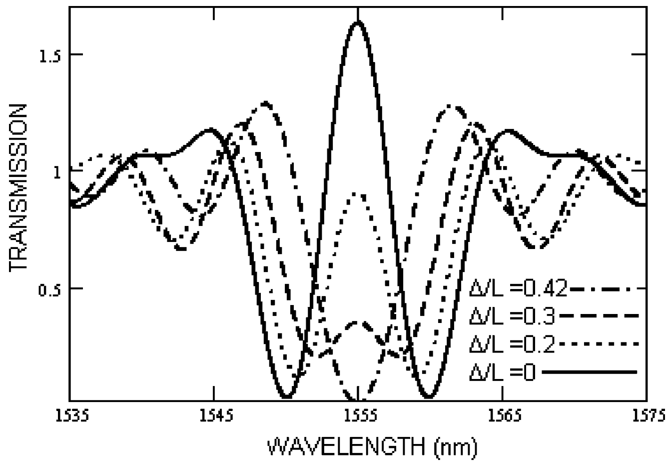

Fig. 11. Transmission spectra of the filter with the π-shifted TG for $L = 50$ mm; $\alpha_2 = -20.4\ \mathrm{m}^{-1}$; $\kappa = 31.4\ \mathrm{m}^{-1}$ for different distances of the π-shift from the TG center: $\Delta/L = 0$ (solid); $\Delta/L = 0.2$ (dotted); $\Delta/L = 0.3$ (dashed); $\Delta/L = 0.42$ (dotted–dashed).

gradually tuned from 2.1 dB of amplification to -30 dB of attenuation.

B. Spectrally Nonuniform Gain/Loss

The assumption of a uniform gain spectrum works well for narrow-band Bragg gratings, however, in the case of TGs with generally much broader transmission spectrum, gain, as well as loss, may have a significant dependence on wavelength. The relationship between the real and imaginary parts of a mediums complex ionic susceptibility associated with a resonant absorption transition is governed by the well-known Kramers-Kronig equations. For a medium with refractive index n_0 into which a dopant with susceptibility $|\chi(\omega)| \ll 1$ is introduced, the refractive index $\mathrm{n}(\omega)$ and absorption coefficient $\alpha(\omega)$ are given by

$$n(\omega) \approx n_0 + \frac{\chi'(\omega)}{2n_0}$$
$$\alpha(\omega) \approx -\frac{\omega}{n_0 c_0}\chi''(\omega) \tag{15}$$

where c_0 is the speed of light in vacuum. Spectral distribution of the ionic susceptibility of erbium-doped fiber can be presented as $\chi(\lambda)$ and can be approximated by complex Lorenz functions [34].

We calculated the gain/loss coefficient spectra from linear combinations of the gain and absorption data in the following ratios: 0:100, 20:80, and 100:0 (i.e., unpumped, partial inversion and full inversion). The maximum loss/gain at 1532-nm peak was 2 dB/cm. The calculated variation of the refractive index turned out to be $\delta n < 1.5\ 10^{-6}$. The variation of the refractive index would be significant for the TG spectrum, if $\delta n > \delta\lambda/\Lambda$, where $\delta\lambda$ is the characteristic wavelength scale of the TG spectral features and Λ its period. For typical values of $\delta\lambda \sim 2$ nm and $\Lambda \sim 220\ \mu$m, we get maximum allowed index change $\sim 10^{-5}$, which is much larger than the variation of the refractive index due to erbium absorption or gain. Therefore, the only effect of the gain spectral nonuniformity on the TG spectrum would be due to amplifying or attenuating specific wavelengths depending on the values of the material absorption and gain. Equations (1)–(14) will be still valid, but with the constant gain/loss parameter α_2 replaced by $\alpha_2(\lambda)$.

C. Spatially Nonuniform Gain/Loss

Finally, we consider how transmission would be affected by spatial nonuniformity of the gain/loss. The gain/loss is spatially uniform only for the two extreme situations: unpumped, and strongly pumped to $+100\%$ inversion all along the TG. For the intermediate states, the pump light intensity is reduced along the TG, due to absorption, creating a gain/loss nonuniformity. We estimated the effect of this nonuniformity by integrating (1) and found no substantial spectrum distortions as the inversion increased. Unlike the case of spectral gain/loss nonuniformity, where it affects particular spectral components of the transmission spectrum, the spatial nonuniformity has the effect of being integrated: it is important only how much gain/loss is accumulated over the grating length.

VI. Conclusion

The lossy nature of cladding layers in waveguide structures and specially designed fibers plays a very important role in the spectral behavior of a transmission grating, such as LPG. An understanding of how these loss or gain in waveguide modes affects the grating spectral characteristics enables improved grating design and invites much potential for dynamically controlled filtering characteristics. We have demonstrated that certain levels of losses in the cladding modes lead to distinct behavior of LPGs as band rejection filters and sensing elements. By keeping the proper loss-to-coupling or gain-to-coupling ratio, virtually complete attenuation of the core mode can be achieved at the resonance wavelength for any value of the grating strength κL. This is impossible for traditional, loss-free or low-loss LPGs, in which complete energy transfer to the cladding is only achieved at fixed values of the grating strength $(\kappa L > (m + 1/2)\pi)$. In contrast to loss-free uniform LPGs, those featuring optimized loss levels provide transmission spectrum with slightly wider bandwidth of side-lobe-free tails. Once the optimum level of losses for 100% attenuation is set for the chosen value of the grating strength, the LPG preserves a Gaussian-like, side-lobe free transmission spectrum for any value of the LPG length and the coupling coefficient.

We also demonstrated that the attenuation/amplification level can be controlled by introducing π-shift along the grating. This type of control can be combined with the pump control in planar waveguides based on rare-earth-doped electro-optic polymers. Not only π-shift position, but also the length and the coupling coefficient of the grating could be controlled in these types of devices. It was also demonstrated that wavelength dependence of the gain in Er-doped fibers factor does not lead to severe spectrum distortions in the case of erbium-doped waveguides.

References

[1] J. J. Pan, K. Guan, X. Qiu, W. Wang, M. Zhang, J. Jiang, E. Zhang, and F. Q. Zhou, "Advantages of low-cost, miniature, intelligent EDFAs for next-generation dynamic metro/access networks," *Opt. Fiber Technol.*, vol. 9, pp. 80–94, 2003.

[2] Z. Wang, T. Durhuus, B. Mikkeleson, and K. E. Stubkjaer, "Distributed feedback laser amplifiers combining the functions of amplifiers and channel filters," *Appl. Phys. Lett.*, vol. 64, pp. 2065–2067, 1994.

Authorized licensed use limited to: McGill University. Downloaded on February 23,2010 at 11:27:11 EST from IEEE Xplore. Restrictions apply.

[3] T. Erdogan, "Fiber grating spectra," *J. Lightwave Technol.*, vol. 15, pp. 1277–1294, July 1997.
[4] A. M. Vengsarkar, P. J. Lemaire, J. B. Judkins, V. Bhatia, T. Erdogan, and J. E. Sipe, "Long-period fiber gratings as band-rejection filters," *J. Lightwave Technol.*, vol. 14, pp. 58–65, Jan. 1996.
[5] V. Grubsky, D. S. Starodubov, and J. Feinberg, "Wavelength-selective coupler and add-drop multiplexer using long-period fiber gratings," in *Proc. OFC* , 2000, pp. 28–30.
[6] H. J. Patrick, A. D. Kersey, and F. Bucholtz, "Analysis of the response of long-period gratings to external index of refraction," *J. Lightwave Technol.*, vol. 16, pp. 1606–1612, Sept. 1998.
[7] Q. Li, A. A. Au, C.-H. Lin, E. R. Lyons, and H. P. Lee, "An efficient all-fiber variable optical attenuator via acoustooptic mode coupling," *IEEE Photon. Technol. Lett.*, vol. 14, pp. 1563–1565, Nov. 2002.
[8] S. Ramachandran, M. F. Yan, E. Monberg, F. V. Dimarcello, P. Wisk, and S. Ghalmi, "Record bandwidth, spectrally flat coupling with microbend gratings in dispersion-tailored fibers," *IEEE Photon. Technol. Lett.*, vol. 15, pp. 1561–1563, Nov. 2003.
[9] X. Shu, L. Zhang, and I. Bennion, "Sensitivity characteristics of long-period fiber gratings," *J. Lightwave Technol.*, vol. 20, pp. 255–266, Feb. 2002.
[10] D. B. Stegall and T. Erdogan, "Leaky cladding mode propagation in long-period fiber gratings devices," *IEEE Photon. Technol. Lett.*, vol. 11, pp. 343–345, Mar. 1999.
[11] X. Daxhelet and M. Kulishov, "Theory and practice of long-period gratings: when a loss becomes a gain," *Opt. Lett.*, vol. 28, pp. 686–688, 2003.
[12] D. An, Z. Yue, and R. T. Chen, "Dual-functional polymeric waveguide with optical amplification and electro-optic modulation," *Appl. Phys. Lett.*, vol. 72, pp. 2806–2808, 1998.
[13] I. Baumann, S. Bosso, R. Brinkmann, R. Corsini, M. Dinand, A. Greiner, K. Schäfer, J. Söchtig, W. Sohler, H. Suche, and R. Wessel, "Er-doped integrated optical devices in LiNbO3," *IEEE J. Select. Topics Quantum Electron.*, vol. 2, pp. 355–366, June 1996.
[14] H. Ma, A. K.-Y. Jen, and L. R. Dalton, "Polymer-based optical waveguides: materials, processing and devices," *Adv. Mater.*, vol. 14, pp. 1339–1365, 2002.
[15] G. Karve, B. Bihari, and R. T. Chen, "Demonstration of optical gain at 1.06 μm in a neodymium-doped polyimide waveguide," *Appl. Phys. Lett.*, vol. 77, pp. 1253–1255, 2000.
[16] G. G. Karapetyan, A. V. Daryan, D. M. Meghavoryan, and N. E. Gevoryan, "Theoretical investigation of active fiber Bragg grating," *Opt. Commun.*, vol. 205, pp. 421–425, 2002.
[17] V. E. Kochergin and E. V. Kochergin, "Optical tunneling through fiber Bragg grating with gain," *Opt. Commun.*, vol. 211, pp. 121–128, 2002.
[18] H. V. Baghdasaryan and T. M. Knyazyan, "Simulation of amplifying phase-shifted fiber Bragg gratings by the method of single expression," *Opt. Quantum Electron.*, vol. 35, pp. 493–506, 2003.
[19] V. Rastogi, "Long-period gratings in planar optical waveguides," *Appl. Opt.*, vol. 41, pp. 6351–6355, 2002.
[20] Y. B. Lu and P. L. Chu, "Gain flattening by using dual-core fiber in Erbium-doped fiber amplifier," *IEEE Photon. Technol. Lett.*, vol. 12, pp. 1616–1618, Dec. 2000.
[21] K. Thyagarajan and J. K. Anad, "A novel design of an intrinsically gain-flattened erbium doped fiber," *Opt. Commun.*, vol. 183, pp. 407–413, 2000.
[22] S. Woods, "Specialty-fiber innovations benefit fiber lasers," *Laser Focus World*, pp. 85–88, June 2003.
[23] L. J. A. Nilsson, D. C. Hanna, J. D. Minelly, and R. E. Paschotta, "Optical Amplifier and Light Source," U.S. Patent 6 445 494, Sept. 3, 2002.
[24] J. P. Koplow, S. W. Moore, and D. A. V. Kliner, "A new method for side pumping of double-cladd fiber sources," *IEEE J. Quantum. Electron.*, vol. 39, pp. 529–540, Apr. 2003.
[25] A. W. Snyder and J. D. Love, *Optical Waveguide Theory*. London, U.K.: Chapman and Hall, 1983.
[26] R. R. A. Syms, S. Makrimichalou, and A. S. Holms, "High-speed optical signal processing potential of grating-coupled waveguide filters," *Appl. Optics*, vol. 30, pp. 3762–3769, 1991.
[27] G. Lenz, B. J. Eggleton, C. R. Giles, C. K. Madsen, and R. E. Slusher, "Dispersive properties of optical filters for WDM systems," *IEEE J. Quantum Electron.*, vol. 34, pp. 1390–1401, Aug. 1998.
[28] D. S. Starodubov, V. Grubsky, and J. Feinberg, "All-fiber bandpass filter with adjustable transmission using cladding-mode coupling," *IEEE Photon. Technol. Lett.*, vol. 10, pp. 1590–1592, Nov. 1998.
[29] B. C. Hwang, S. Jiang, T. Luo, K. Seneschal, G. Sorbello, M. Morrell, F. Smektala, S. Honkanen, J. Lukas, and N. Peyghambarian, "Performance of high-concentration Er^{3+}-doped phosphate fiber amplifiers," *IEEE Photon. Technol. Lett.*, vol. 13, pp. 197–199, Mar. 2001.
[30] Y.-H. Jan, M. E. Heimbuch, L. A. Coldren, and S. P. DenBaars, "InP/GaAsP grating-assisted codirectional coupler tunable receiver with a 30 nm wavelength tuning range," *Electron. Lett.*, vol. 32, pp. 1697–1699, 1996.
[31] M. Kulishov, X. Daxhelet, M. Mounir, and M. Chaker, "Electronically reconfigurable superimposed waveguide long-period gratings," *J. Opt. Soc. Amer. A*, vol. 19, pp. 1632–1648, 2002.
[32] H. Ke, K. S. Chiang, and J. H. Peng, "Analysis of phase-shifted long-period fiber gratings," *IEEE Photon. Technol. Lett.*, vol. 10, pp. 1596–1598, Nov. 1998.
[33] M. Kulishov and X. Daxhelet, "Reconfigurable π-shifted and Mach-Zehnder bandpass filters on the basis of electro optically induced long-period gratings in a planar waveguide," *J. Lightwave Technol.*, vol. 21, pp. 854–861, Mar. 2003.
[34] F. Matera, M. Romagnoli, M. Settembre, and M. Tamburrini, "Evaluation of chromatic dispersion in erbium doped fiber amplifiers," *Electron. Lett.*, vol. 27, pp. 1687–1689, 1991.

Mykola Kulishov received the M.S. degree in radiophysics from Kyiv State University, Kyiv, Ukraine, in 1978, and the Ph.D. degree in optoelectronics from the Institute of Cybernetics, Ukrainian Academy of Sciences, Kyiv, in 1993.

He is currently with Adtek Photomask Inc., Montreal, QC, Canada. His research interests include tuneable fiber-optic components, optical waveguides, integrated optics, and reconfigurable optical filters.

Victor Grubsky received the M.S. degree in physics from the Moscow Institute of Physics and Technology, Russia, in 1995, and the Ph.D. degree in physics from the University of Southern California, Los Angeles, in 1999.

He was a member of the founding team of Sabeus Photonics, where he worked from 1998 to 2004 as a Vice-President of Research and Development. He was involved in the development of fiber-optic components for telecom and sensor applications. He was the inventor of the precise passive filter technology based on long-period fiber gratings, and a co-inventor of the award-winning technology for noninvasive manufacturing of Bragg gratings with near-UV light. Currently, he is with the University of Southern California. His research interests are related to optical waveguide properties, such as nonlinear effects in fibers, mode-converting devices, waveguide gratings, and fiber lasers.

Joshua Schwartz (S'00) received the B.S. (Hons.) degree from McGill University, Montreal, QC, Canada, where he is currently pursuing the Ph.D. degree.

He is working under the supervision of David Plant, gaining experience with long period gratings and waveguide characterization. He has also recently published his undergraduate research on chip-to-chip free-space optical links.

Xavier Daxhelet was born in Mouscron, Belgium, in 1964. He received the B.S. degree in mathematic physics from the University of Montreal, Montreal, QC, Canada, in 1987, and the Ph.D. degree in engineering physics from the Ecole Polytechnique de Montreal, Montreal, QC, Canada, in 1990.

He is currently a Research Fellow with the Ecole Polytechnique de Montreal. His main interests are all-fiber components such as fused couplers, Bragg gratings, and tapered fibers.

David V. Plant (S'86–M'89) received the Ph.D. degree in electrical engineering from Brown University, Providence, RI, in 1989.

From 1989 to 1993, he was a Research Engineer in the Department of Electrical and Computer Engineering, University of Southern California, Los Angeles. In 1993, he joined the Department of Electrical and Computer Engineering, McGill University, Montreal, QC, Canada, as an Assistant Professor, was promoted to Associate Professor 1997 and to Professor in 2004. During the 2000–2001 academic year, he went on leave from McGill to become the Director of Optical Integration at Accelight Networks, Pittsburgh, PA. He is the Principle Investigator (PI) and Scientific Director of the NSERC funded Agile All-Photonic Networks (AAPN) research program, and the PI and Center Director of the Quebec-funded Center for Advanced Systems and Technologies in Communications.

Dr. Plant has received numerous awards, most recently the Carrie M. Derick Award for Graduate Student Supervision, Teaching, and Research in 2004 and was named a James McGill Professor in 2001.

Authorized licensed use limited to: McGill University. Downloaded on February 23,2010 at 11:27:11 EST from IEEE Xplore. Restrictions apply.